ORIGINAL ARTICLE

Mathematical models and simulations of phase noise in phase-locked loops

Sethapong Limkumnerd[1] and Duangrat Eungdamrong[2]

Abstract

Limkumnerd, S. and Eungdamrong, D.
Mathematical models and simulations of phase noise in phase-locked loops
Songklanakarin J. Sci. Technol., 2007, 29(4) : 1017-1028

Phase noises in Phase-Locked Loops (PLLs) are a key parameter for communication systems that contribute the bit-rate-error of communication systems and cause synchronization problems. Accurate predictions of phase noises through mathematical models are consequently desirable for practical designs of PLLs. Despite many phase noise models derived from noise sources from electronic devices such as an oscillator and a multiplier have been proposed, no phase noise models that include noises from loop filters have specifically been investigated. This paper therefore investigates the roles of loop filters in phase noise contribution. The major scopes of this paper is a detailed analysis and simulations of phase noise models resulting from all components. i.e. a voltage-controlled oscillator, a multiplier and a filter. Two particular second-order passive and active low-pass filters are compared. The results show that simulations of phase noises without an inclusion of filter noises may not be accurate because the filter noises, particularly the active filter, significantly contribute the total phase noise. Moreover, the passive filter does not significantly dominate the phase noise at low offset frequency while the active filters entirely dominate. Therefore, the passive filter is a more efficient filter for PLL circuit at low offset frequency. The phase noise models presented in this paper are relatively simple and can be used for accurate phase noise prediction for PLL designs.

Key words : phase-locked-loop, phase noise, voltage control oscillator, phase detector, loop filter, main divider

[1]M.Sc. student in Telecommunication, [2]Ph.D.(Electrical and Computer Engineerging), Asst. Prof., School of Communications Instrumentations and Control Sirindhorn International Institute of Technology, Thammasat University, 131 Moo 5, Tiwanont Road, Bangkadi, Muang, Pathum Thani, 12000 Thailand.
Corresponding e-mail: thanyee@yahoo.com
Received, 28 November 2006 Accepted, 28 February 2007

บทคัดย่อ

เศรษฐพงษ์ หลิมกำเนิด และ ดวงรัตน์ อึ๊งดำรง

การจำลองแบบสัญญาณรบกวนเฟสในวงจรเฟสล็อกลูปด้วยแบบจำลองทางคณิตศาสตร์

ว. สงขลานครินทร์ วทท. 2550 29(4) : 1017-1028

สัญญาณรบกวนเฟสเป็นตัวชี้วัดสมบัติสำคัญของวงจรเฟสล็อกลูปในระบบการสื่อสาร เนื่องจากเป็นสาเหตุหลักของความผิดพลาดของชุดข้อมูลและกระบวนการซินโครไนซ์สัญญาณ ดังนั้นการทำนายระดับสัญญาณรบกวนเฟสด้วยแบบจำลองทางคณิตศาสตร์จึงเป็นขั้นตอนสำคัญสำหรับการออกแบบวงจรเฟสล็อกลูปที่มีความแม่นยำสูง การศึกษาแบบจำลองทางคณิตศาสตร์ของสัญญาณรบกวนเฟสที่นำเสนอก่อนหน้านี้มิได้ศึกษารวมไปถึงวงจรกรองสัญญาณ ซึ่งเป็นแหล่งกำเนิดสัญญาณรบกวนที่สำคัญอีกส่วนหนึ่ง ภายในบทความนี้จึงนำเสนอแบบจำลองทางคณิตศาสตร์ของสัญญาณรบกวนเฟสทั้งระบบ ซึ่งประกอบด้วย วงจรกำเนิดสัญญาณ วงจรหาร วงจรคูณและวงจรกรองสัญญาณ โดยเฉพาะอย่างยิ่งได้นำเสนอแปรียบเทียบคุณสมบัติวงจรกรองสัญญาณแบบแอกทีฟและแพสซีฟด้วย จากการจำลองการทำงานพบว่าการใช้วงจรกรองแบบแพสซีฟมีค่าสัญญาณรบกวนเฟสน้อยกว่าแบบแอกทีฟที่ความถี่ออฟเซตต่ำและแบบจำลองทางคณิตศาสตร์สามารถทำนายสัญญาณรบกวนเฟสได้อย่างครบถ้วน ดังนั้นแบบจำลองทางคณิตศาสตร์ที่นำเสนอจึงสามารถนำไปใช้ในการออกแบบแบบวงจรเฟสล็อกลูปที่มีความแม่นยำสูงได้

ภาควิชาการสื่อสาร อุปกรณ์วัดและระบบควบคุม สถาบันเทคโนโลยีนานาชาติสิรินธร มหาวิทยาลัยธรรมศาสตร์ 131 หมู่ 5 ถนนติวานนท์ ศูนย์บางกะดี ตำบลบางกะดี อำเภอเมือง จังหวัดปทุมธานี 12000

Phase Locked Loops (PLLs) are extensively used for a variety of radio applications such as in frequency synthesizers or in carrier recovery and clock recovery circuits (Lathi, 1998). Such PLLs are closed-loop systems that utilize a negative feedback to sustain a constant ratio of an output frequency to an input frequency (Rohde, 1997). Generally, desirable performances of PLLs are not only high frequency but also low phase noise (Rohde *et al.*, 2005). The high frequency operations can be achieved through the use of high transition frequency (f_T) technologies such as Bipolar or BiCMOS devices. However, the phase noises have significantly degraded the performances of PLLs by reducing the signal-to-noise ratio (SNR), increasing adjacent channel power and reducing adjacent channel rejection (Kroupa, 2003). As a result, the degraded performances of the PLLs contribute the bit-rate-error of communication systems and cause synchronization problems in clocked and sampled data digital systems (Misra, 2001).

Consequently, predicting phase noise through mathematical models and simulations are important before practical implementations. Despite Leeson's Equation (1966) being first recognized as a classical phase noise prediction in PLLs, such equation predicts only the single-sideband phase noise measured from the power spectral density of the carrier and an amplitude variation may also be included. Moreover, calculating phase noise using Leeson's equation requires not only operation of all linear device but also an oscillator that contains only a single resonator (Razavi, 2001). Recently, Ducker (2000) has proposed mathematical models of double-sideband phase noise through two major noise sources, i.e. voltage-controlled oscillator and multiplier. Although Eric Ducker's equations are relatively simple for phase noise prediction, noise models of loop filter have not yet been studied.

As loop filters can be of various types and orders, they may significantly generate noises leading to the total phase noise of PLLs and this paper therefore investigates the roles of loop filters in phase noise contribution through mathematical models and simulations. The major scope of this paper is a detailed analysis and simulations of

phase noise models resulting from all components. i.e. a voltage-controlled oscillator, a multiplier and using MATHEMATICA and MATLAB. Two particular second-order passive and active low pass filters are compared. The paper is organized as follows; Section 1 commences by literature reviews on basic PLLs. Sections 2 and 3 then describe practical effects of phase noise in the frequency domain and mathematical noise models of all components, respectively. Finally, total phase noises of PLLs are summarized and simulated in sections 4 and 5.

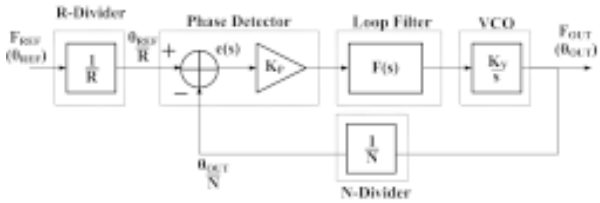

Figure 1. Block diagrams of the basic phase lock loop.

1. PLL Basics

1.1 General Descriptions

Figure 1 shows the block diagrams of a basic PLL. It can be seen from Figure 1 that the PLL is a closed-loop system and consists mainly of five components, i.e. a phase detector (PD), a loop filter, a voltage-controlled oscillator (VCO) and dividers (Dai and Harjani, 2002; Shu *et al.*, 2004). Firstly, the PD is typically a two-input and one-output device that can be realized by a specialized mixer. This PD comes in many configurations including those with logic level inputs, passive and active analog versions, and sampling versions specifically used for high frequency multiplications. Secondly, the loop filter is a low-frequency circuit that filters the phase detector error voltage with which it controls the VCO frequency. Although it can be active or passive, it is usually analog and very simple. In extreme cases, it might be an entire microprocessor. Thirdly, the VCO is the control element for a PLL in which the output frequency changes correspondingly with the tuning voltage. Finally, the N and R dividers are devices that convert a high output frequency and a reference frequency, respectively, to a low frequency for a multiplication process at the PD.

With reference to Figure 1, the loop gain L(s) (Thamsirianunt and Kwasniewski, 1997) in s-domain can be expressed by a multiplication between a forward loop gain $G(s) = K_pK_vF(s)/s$ and a reverse loop gain $H(s) = 1/N$ as

$$L(s) = G(s) \times H(s) = \frac{1}{s}\left(\frac{K_p \times K_v \times F(s)}{N} \right) \quad (1)$$

where K_p is a phase gain of the PD, K_v is a voltage control sensitivity of the VCO and F(s) is the transfer function of a loop filter. The consequent closed loop transfer functions are generally described separately for each component as will be seen later in section 4.

1.2 Operations

The operations of The PLL can be described in terms of a reference phase Φ_{REF} and an output phase Φ_{OUT} as follows Zhang *et al.*(2003). When Φ_{OUT} Φ_{REF}, the PD compares the phases between the output phase Φ_{OUT}/N and the reference phase Φ_{REF}/R and hence generates an error voltage e(s). In other words,

$$e(s) = \frac{\Phi_{REF}}{R} - \frac{\Phi_{OUT}}{N} \quad (2)$$

The derivative of Equation (2) yields

$$\frac{d[e(s)]}{dt} = \frac{F_{REF}}{R} - \frac{F_{OUT}}{N} \quad (3)$$

Typically, the error voltage e(s) in Equation (2) subsequently enters the VCO as a control voltage and must remain constant. Such error voltage e(s), however, consists of both DC and high-frequency components and the filtering process is significantly required. Therefore, the e(s) is then filtered through the lowpass filter with a transfer function F(s) for suppressing the high-frequency components of the PD and presenting only the DC level for the oscillator. If the loop

gain is large enough, the error e(s) becomes a very small value in steady state or is almost constant. Equation (3) is consequently equal to

$$\frac{d[Constant]}{dt} = 0 = \frac{F_{REF}}{R} - \frac{F_{OUT}}{N} \quad (4)$$

Thus,

$$F_{OUT} = \left(\frac{N}{R}\right) F_{REF} \quad (5)$$

When the PLL is locked, it produces an output that has a small and constant phase error with respect to the input phase but the output frequency is the same or linearly proportional to the reference frequency as shown in Equation (5).

2. Phase Noise Analysis

Phase noise is widely used to describe the characteristic randomness of frequency stability. Generally, two types are single- sideband $L(f_m)$ or double sideband $S_\Phi(f_m)$ phase noises. On the other hand, the $L(f_m)$ can directly be measured through the power spectral density (PSD) of the signal using the spectral analyzer at RF with a 1-Hz resolution-bandwidth filter. Figure 2 shows the measured PSD of the carrier power and the single-sideband phase noise power. As shown in Figure 2, the $L(f_m)$ (Manassewitsch, 1987) can be described in decibels relative to the carrier level as dBc/Hz as the ratio of the noise power at an offset frequency f_m from the carrier (P_{SSB}) to the carrier power (P_C). In other words,

Single – Sideband Phase Noise =

$$10\log(L(f_m)) = 10\log\left(\frac{P_C}{P_{SSB}}\right) \quad (6)$$

On the other hand, the $S_\Phi(f_m)$ can be measured through the PSD of the modulation of signal with the ideal phase modulator using the spectrum analyzer at RF with a 1-Hz resolution-bandwidth. Note that the $S_\Phi(f_m)$ is twice (3-dB more than) the $L(f_m)$. Figure 3 shows plots of the $S_\Phi(f_m)$ versus the log scale of the offset frequency f_m consequently demonstrating the nonlinear decay and demon-strates various regions of the phase noise depend-ing on the regions of slopes. Table 1 summarizes types and slopes of noises in each region. The $S_\Phi(f_m)$ can be described in dBc/Hz as a general phase noise equation that includes the noises in all regions of slopes as summarized in Table 1. In other words,

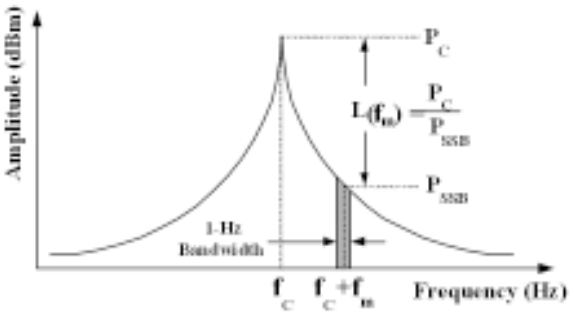

Figure 2. Power spectral density of the carrier power and the single-sideband noise power.

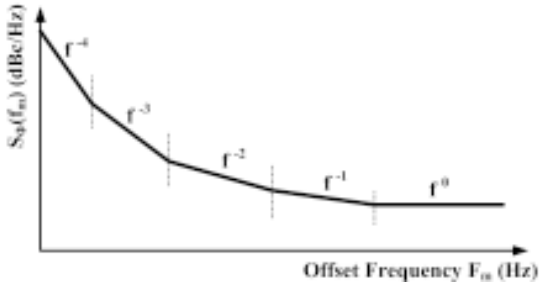

Figure 3. Plots of double-sideband phase noises in dBc/Hz versus offset frequency f_m in Hz.

Table 1. Summary of types and slopes of noises in each region.

Regions	Coefficients	Types of Noise	Slopes (dB)
$1/f^0$	k_0	White Noise	0
$1/f^1$	k_1	Flicker Noise	-10
$1/f^2$	k_2	White FM	-20
$1/f^3$	k_3	Flicker FM	-30
$1/f^4$	k_4	Random Walk FM	-40

Double - Sideband Phase Noise =

$$S_{\Phi}(f_m) = 10\log\left(\frac{k_0}{f^0} + \frac{k_1}{f^1} + \frac{k_2}{f^2} + \frac{k_3}{f^3} + \frac{k_4}{f^4}\right) \quad (7)$$

where f is a frequency in Hz (Manassewitsch, 1987). Consequently, mathematical models of noise sources in this paper are based on the double sideband phase noise equation shown in Equation (7).

3. Mathematical Noise Source Models

3.1 Typical Noise Models for VCO and Multiplier

Figure 4 shows the block diagram of a basic PLL with an inclusion of three noise models, i.e. a noise model for the VCO $N_{VCO}(f)$, a noise model for multiplier $N_{MUL}(f)$ and noise models $N_{FIL1}(f)$ and $N_{FIL2}(f)$ for passive filter and active filters, respectively. With reference to Figure 4, noise models for $N_{VCO}(f)$ and $N_{MUL}(f)$ are common and described as follows. The noise model of $N_{VCO}(f)$ is given by

$$N_{VCO}(f) = k_{0\_VCO} + \frac{k_{2\_VCO}}{f^2} + \frac{k_{3\_VCO}}{f^3} \quad (8)$$

where k_{0_VCO}, k_{2_VCO}, k_{3_VCO} are coefficients of white, white FM and flicker FM noises in the VCO, respectively. On the other hand, the noise model $N_{MUL}(f)$ can be expressed in terms of the noise models of the dividers and the reference oscillator for simplicity as (Ducker, 2000)

$$N_{MUL}(f) = N^2\left[\left(k_{0\_md} + \frac{k_{1\_md}}{f}\right) + \left(\frac{k_{0\_ref} + \frac{k_{1\_ref}}{f} + \frac{k_{2\_ref}}{f^2} + \frac{k_{3\_ref}}{f^3}}{R^2}\right)\right] \quad (9)$$

where k_{0_md} and k_{1_md} are coefficients of white and flicker noises in the main divider, respectively. In addition, k_{0_ref}, k_{2_ref}, k_{3_ref} and k_{4_ref} are coefficients of white, flicker, white FM and flicker FM noises in the reference oscillator, respectively. However, the noise model of the loop filter is not typically specified depending on the types of filters. Therefore, the noises models of $N_{FIL1}(f)$ and $N_{FIL2}(f)$ are particularly analyzed and compared as follows.

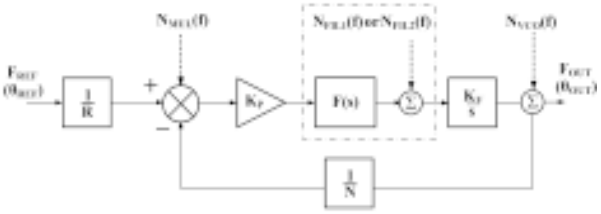

Figure 4. Block diagrams of the basic phase lock loop with an inclusion of noise sources.

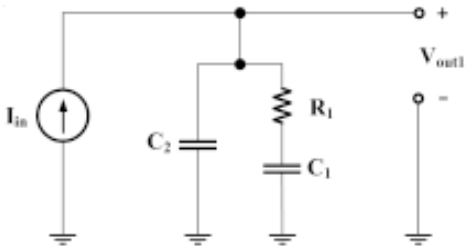

Figure 5. Circuit configurations of the second-order passive lowpass filter F_1.

3.2 Noise Model $N_{FIL1}(f)$ of Passive Filter F_1

Figure 5 shows the circuit configurations of a second-order passive lowpass filter F_1. As shown in Figure 5, the circuit is relatively simple and are formed a single resistor R_2 and two capacitors C_2 and C_3. The transfer function $F_1(s)$ in s-domain can be described in terms of an output voltage V_{out} and an input current I_{in} as follows

$$F_1(s) = \frac{V_{out1}(s)}{I_{in}(s)} = \frac{1 + sR_1C_1}{s(C_1 + C_2)\left(1 + \frac{sR_1C_1C_2}{C_1 + C_2}\right)} \quad (10)$$

In other words,

$$F_1(s) = \frac{k_{F1}\left(1 + s\tau_{F1\_1}\right)}{s\left(1 + s\tau_{F1\_2}\right)} \quad (11)$$

where $k_{F1} = 1/(C_1+C_2)$ is a constant. $\tau_{F1\_1} = R_1C_1$ and $\tau_{F1\_2} = (R_1C_1C_2)/(C_1+C_2)$ are time constants. Analytical treatments for $F_1(s)$ are shown in

Appendix A.1. In addition to the transfer function, the noises in the filter F_1 may come from both capacitor and resistor. As the capacitor does not significantly contribute noises, the noise of the loop filters are therefore mainly from the resistor R_1. Typically, noise in resistor results from a random motion of electrons in the resistor. The noise model for a resistor $P_r(R)$ is assumed to be white noise and is equal to 4kTBR where k is the Boltzmann's constant, T is an absolute temperature in [K], B is a bandwidth of the filter in [Hz] and R is an actual value of the resistor in [Ω]. Such $P_r(r)$ is also a power dissipated by the resistor and commonly known as a thermal noise. As a result, the noise model of the resistor dominates the passive filter F_1 and the can be described as $N_{FIL1}(f) = P_r(R) =$ 4kTBR (Kroupa, 2003). In other words,

$$N_{FIL1}(f) = k_{0\_R} \tag{12}$$

where k_{0_R} is a coefficient of the white noise contributed by the resistor in the passive filter F_1.

3.3 Noise Model $N_{FIL2}(f)$ of Active Filter F_2

Figure 6 shows the circuit configurations of a second-order active lowpass filter F_2. As shown in Figure 6, the circuit mainly consists of the operational amplifier (Op-Amp), two resistors R_1 and R_2, and two capacitors C_1 and C_2. The transfer function $F_2(s)$ in s-domain can be described in terms of an output voltage V_{out} and an input voltage V_{in} as follows

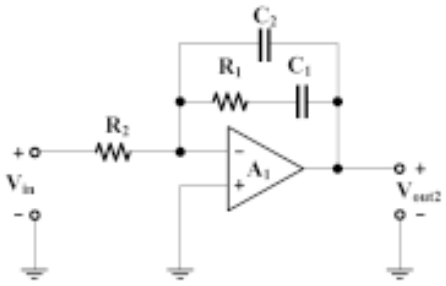

Figure 6. Circuit configurations of the second-order active lowpass filter F_2.

$$F_2(s) = \frac{V_{out2}(s)}{V_{in}(s)} = \frac{1 + sR_1C_1}{sR_2(C_1 + C_2)(1 + \frac{sR_1C_1C_2}{C_1 + C_2})} \tag{13}$$

In other words,

$$F_2(s) = \frac{\left(1 + s\tau_{F2\_1}\right)}{s\tau_{F2\_3}\left(1 + s\tau_{F2\_2}\right)} \tag{14}$$

where $\tau_{F2\_1} = R_1C_1$, $\tau_{F2\_2} = (R_1C_1C_2)/(C_1+C_2)$ and $\tau_{F2\_3} = R_2(C_1+C_2)$ are time constants in addition the DC gain of the active filter can be determined by the integrator term, i.e $k_{F2} = 1/R_2(C_1+C_2)$. Analytical treatments for $F_2(s)$ are shown in Appendix A.2. In terms of noise contributions, it can be seen from Figure 5 that the noise sources result from not only resistors as previously described in Equation (12) but also the Op-Amp. Generally, the noise from the Op-amp includes the flicker and the thermal noises and is derived by experiments or given by the manufacturer. Consequently, the noise model for the active filter F_2 is given by

$$N_{FIL1}(f) = k_{0\_R} + k_{0\_OA} + \frac{k_{1\_OA}}{f} \tag{15}$$

where k_{0_OA} and k_{1_OA} are coefficients of the white and flicker noises contributed by the operational amplifier in the active filter F_2.

4. Mathematical Phase Noise Models

4.1 Typical Phase Noise Models for VCO and Multiplier

Typically, output phase noise ($S_\Phi(f)$) of each noise source can be modeled by a multiplication between an input power spectral density and a squared magnitude of a closed loop transfer function ($\theta(s)$) in which the input is varied depending on the investigated noise sources. In other words,

$$S_\Phi(f) = N(f) \times |\theta(s)|^2 \tag{16}$$

Referring to Figure 4, the closed loop transfer function of the VCO noise is given by

$$\theta_{VCO}(s) = \frac{1}{1+L(s)} \tag{17}$$

Substituting Equations (16) with Equations (8) and (17) yields the phase noise model of the VCO $S_{\Phi\_VCO}(f)$ as

$$S_{\Phi\_VCO}(f) = N_{VCO}(f) \times \left|\theta_{VCO}(s)\right|^2 \tag{18}$$

In addition, the closed loop transfer function for the multiplier is given by

$$\theta_{MUL}(s) = \frac{L(s)}{1+L(s)} \tag{19}$$

Similarly, substituting Equations (16) with Equations (9) and (19) yields the phase noise model of the multiplier $S_{\Phi\_MUL}(f)$ as

$$S_{\Phi\_MUL}(f) = N_{MUL}(f) \times \left|\theta_{MUL}(s)\right|^2 \tag{20}$$

4.2 Phase Noise Model $S_{\Phi\_FIL1}(f)$ of Passive Filter F_1

As shown in Figure 5, the closed loop transfer function for the passive lowpass filter F_1 can be expressed as

$$\theta_{FIL1}(s) = \frac{1}{s}\left(\frac{K_v}{1+L(s)}\right) \tag{21}$$

By substituting Equations (16) with Equations (12) and (21), the phase noise model of the passive lowpass filter F_1($S_{\Phi\_FIL1}(f)$) is given by

$$S_{\Phi\_FIL1}(f) = N_{FIL1}(f) \times \left|\theta_{FIL1}(s)\right|^2 \tag{22}$$

4.3 Phase Noise Model $S_{\Phi\_FIL2}(f)$ of Passive Filter F_2

As the active low pass filter F_2 is formed by resistors, capacitors and Op-Amp, the two major noise sources are therefore contributed by the resistors and the Op-Amp. Therefore, the transfer function of the Op-Amp and the resistor are different. As shown in Figure 4, the closed loop transfer function for the resistor is given by

$$\theta_R(s) = \frac{1}{s}\left(\frac{K_v}{1+L(s)}\right) \times F_2(s) \tag{23}$$

Meanwhile the closed loop transfer function for the Op-Amp is expressed as

$$\theta_{OA}(s) = \frac{1}{s}\left(\frac{K_v}{1+L(s)}\right) \tag{24}$$

By substituting Equations (16) with Equations (15) and (23), the phase noise model of the resistor ($S_{\Phi\_R}(f)$) is given by

$$S_{\Phi\_R}(f) = N_R(f) \times \left|\theta_R(s)\right|^2 \tag{25}$$

Similarly, substituting Equations (16) with Equations (15) and (24) yields the phase noise model of the Op-Amp ($S_{\Phi\_OA}(f)$) as

$$S_{\Phi\_OA}(f) = N_{OA}(f) \times \left|\theta_{OA}(s)\right|^2 \tag{26}$$

As a result, the summation of Equations (25) and (26) yields phase noise model of the active low-pass filter F2 ($S_{\Phi\_FIL2}(f)$) as follows

$$S_{\Phi\_FIL2}(f) = N_R(f) \times \left|\theta_R(s)\right|^2 + N_{OA}(f) \times \left|\theta_{OA}(s)\right|^2 \tag{27}$$

4.4 Total Phase Noise Models

The total phase noise models can be generally determined by the summation of phase noise generated by all components in a PLL. Therefore, the total phase noise model using the second-order passive lowpass filter can be modeled through the summation of phase noise models described in Equations (18), (20) and (22), i.e. $S_{\Phi 1}(f) = S_{\Phi\_VCO}(f) + S_{\Phi\_MUL}(f) + S_{\Phi\_FIL1}(f)$. In other words, such $S_{\Phi 1}(f)$ is described in dBc/Hz as

$$S_{\Phi 1}(f_m) = 10\log(S_{\Phi\_VCO}(f) + S_{\Phi\_MUL}(f) + S_{\Phi\_FIL1}(f)) \tag{28}$$

In the similar manner, the total phase noise model using the second-order active lowpass filter can be

modeled through the summation of phase noise models described in Equations (18), (20) and (27), i.e. $S_{\Phi 2}(f) = S_{\Phi\_VCO}(f) + S_{\Phi\_MUL}(f) + S_{\Phi\_FIL2}(f)$, and is described in dBc/Hz as

$$S_{\Phi 2}(f_m) = 10\log(S_{\Phi\_VCO}(f) + S_{\Phi\_MUL}(f) + S_{\Phi\_FIL2}(f)) \quad (29)$$

5. Simulation Results

Phase noises of the PLL have been simulated using MATHEMATICA and MATLAB. Based on Drucker (2000), Table 2 summarizes values of components of the passive filter F_1 and the active filter F_2 shown in Figures 5 and 6, respectively. In addition, Table 3 also summarizes values of noise coefficients used in simulations by Ducker (2000). For purposes of comparison, both filters F_1 and F_2 have been designed to operate at the same corner frequencies. Figure 7 shows the simulated bode plots of such two filters. Comparisons of calculated and simulated values DC gains and corner frequencies are summarized in Table 4. It can be considered from Table 4 that the corner frequencies of both filters F_1 and F_2 are equal, i.e. $f_{F1\_1} = f_{F2\_1}$ and $f_{F1\_2} = f_{F2\_2}$. However, the DC gain of the filter F_1 is has been constantly fixed while the DC gain of the filter F_2 can be tuned through the corner frequency f_{F2_3} that behaves as an integrator and yields a -20 dB/decade for the DC gain.

Table 2. Summary of values of components of the passive filter F_1 and the active filter F_2.

Components		Values	Units
Resistors	R_1	5.62	kΩ
	R_2	2.94	kΩ
Capacitors	C_1	47	nF
	C_2	6.8	nF

Table 3. Summary of noise coefficients used in simulations.

Components	Constants	Values
VCO	k_{0_VCO}	$10^{-15.5}$
	k_{2_VCO}	10^{-3}
	k_{3_VCO}	$10^{0.7}$
	Kv	10^{7}
Main Divider	k_{0_md}	$10^{-15.5}$
	k_{1_md}	$10^{-12.5}$
	N	1000
Reference Divider	R	10
Reference Oscillator	k_{0_ref}	$10^{-15.8}$
	k_{1_ref}	$10^{-12.7}$
	k_{2_ref}	$10^{-9.86}$
	k_{3_ref}	$10^{-7.82}$
Resistor	k_{0_R1}	$10^{-12.64}$
	k_{0_R2}	$10^{-12.92}$
Op-Amp	k_{0_OA}	$10^{-17.045}$
	k_{1_OA}	$10^{-16.02}$
Phase Detector	K_p	0.5

Figure 8 shows the simulated total phase noise $S_{\Phi 1}(f)$ in [dBc/Hz] versus offset frequency in [Hz], running from 1 Hz to 1 GHz. Such total phase noise $S_{\Phi 1}(f)$ is the sum of $S_{\Phi\_VCO}(f)$, $S_{\Phi\_MUL}(f)$ and $S_{\Phi\_FIL1}(f)$ as described in Equation (28). As shown in Figure 8, the total phase noises can be considered in three regions of offset frequency. First, at the offset frequency lower than approximately 700 kHz, only the multiplier noise dominates the total phase noise while both VCO and filter noises are relatively low at low offset frequency and do not significantly contribute to the total noise. Secondly, between 700-kHz to 100-MHz offset frequency, the filter noise dominates

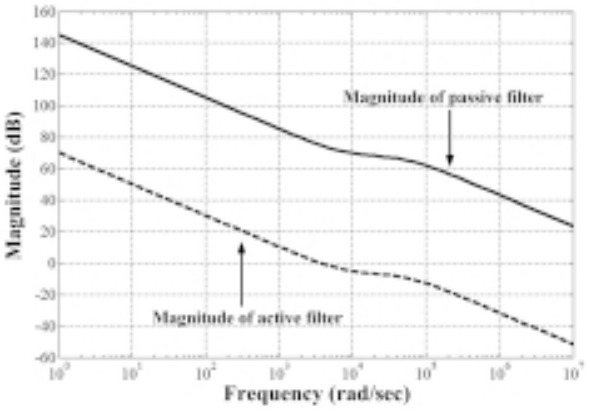

Figure7. Simulated magnitude of filters F_1 and F_2

Table 4. Summary of calculated and simulated values DC gains and corner frequencies of the filters F_1 and F_2.

Filters	Parameters			Values	
				Calculated	Simulated
F_1	DC Gain	k_{F1}	dB	145.38	145.62
	Corner Frequency	$f_{F1\_1} = \omega_{F1\_1}/2\pi = 1/\tau_{F1\_1}$	Hz	7.24×10^3	7.21×10^3
		$f_{F1\_2} = \omega_{F1\_2}/2\pi = 1/\tau_{F1\_2}$	Hz	5.73×10^4	5.74×10^4
F_2	DC Gain	k_{F2}	dB	76.02	76.11
	Corner Frequency	$f_{F2\_1} = \omega_{F2\_1}/2\pi = 1/\tau_{F2\_1}$	Hz	3.31×10^3	3.35×10^3
		$f_{F2\_2} = \omega_{F2\_2}/2\pi = 1/\tau_{F2\_2}$	Hz	7.24×10^3	7.21×10^3
		$f_{F2\_3} = \omega_{F2\_3}/2\pi = 1/\tau_{F2\_3}$	Hz	5.73×10^4	5.74×10^4

the total noise. Finally, at the offset frequency higher than approximately 100 MHz, only the VCO noise dominates.

Figure 9 shows the simulated total phase noise $S_{\Phi 2}(f)$ in [dBc/Hz] versus offset frequency in [Hz], running from 1 Hz to 1 GHz. Such total phase noise $S_{\Phi 2}(f)$ is the sum of $S_{\Phi\_VCO}(f)$, $S_{\Phi\_MUL}(f)$ and $S_{\Phi\_FIL2}(f)$ as described in Equation (29). As shown in Figure 9, the total phase noises can be considered in three regions of offset frequency. First, at the offset frequency lower than approximately 10 Hz, only the multiplier noise dominates the total phase noise while both VCO and filter noises are relatively low at low offset frequency and do not significantly contribute to the total noise. Secondly, between 10-Hz to 800-kHz offset frequency, both the filter noises dominate the total noise. Finally, at the offset frequency higher than approximately 800 kHz, only the VCO noise dominates.

Figure 10 shows the simulated total phase noises of the PLL in dBc/Hz versus offset frequency in [Hz]. As shown in Figure 10, the total phase noise $S_{\Phi 1}(f)$ decreases by -30 dBc/dec in the range of 1 to 35 Hz and gradually decreases until 300 kHz offset frequency before decreasing with the slope to -20 dBc/dec before it reaches the noise floor of -155 dBc at approximately 400 MHz. On the other hand, the total phase noise $S_{\Phi 2}(f)$ starts at -20 dBc/dec at the low offset frequency range

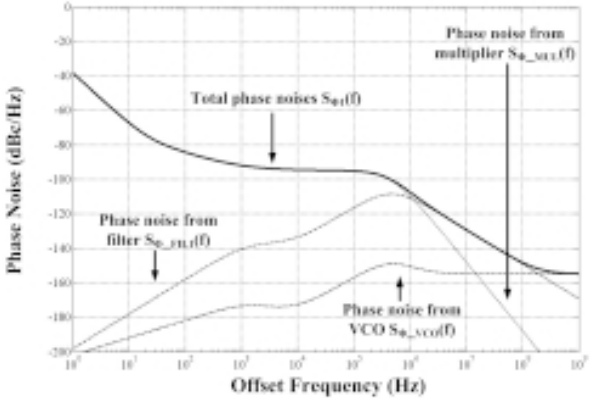

Figure 8. The simulated total phase noise $S_{\Phi 1}(f)$ in [dBc/Hz] versus offset frequency in [Hz].

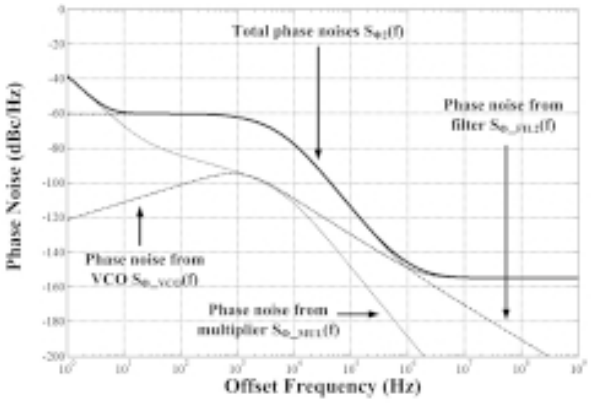

Figure 9. The simulated total phase noise $S_{\Phi 2}(f)$ in [dBc/Hz] versus offset frequency in [Hz].

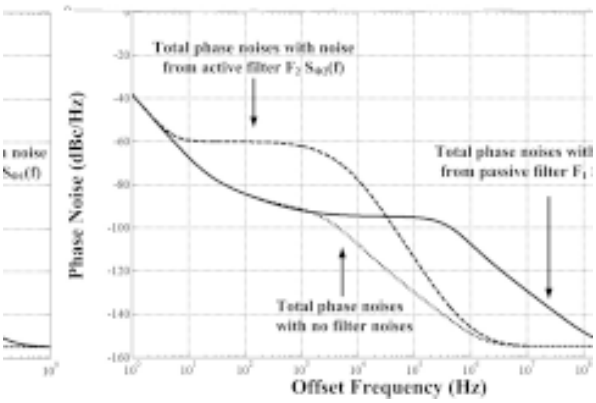

Figure 10. Simulated total phase noises of the PLL in dBc/Hz versus offset frequency in (Hz); (a) the total phase noise $S_{\Phi 1}(f)$ with noises from the passive filter, (b) the total phase noise $S_{\Phi 2}(f)$ with noises from the active filter, (c) the total phase noise with no noises from the filter.

about 1 to 10 Hz. Then the slope remains plateau until it reaches to 1 kHz offset frequency and changes to -40 dBc/dec before it reaches the noise floor of -155 dBc at approximately 10 MHz. In addition, plots of both $S_{\Phi 1}(f)$ and $S_{\Phi 2}(f)$ start at same magnitude of -39 dBc/Hz at 1 Hz offset frequency.

With reference to Figure 10, comparisons between the simulated total phase noise with no filter noises by Ducker (2000) and the simulated total phase noise with passive and active filter noises in this paper have been made. Although the total phase noise without filter noises by Ducker (2000) has shown an excellent performance, this may not be accurate as there was no inclusion of the filter noises. This paper, on the other hand, has shown the effects of filter noises in which accurate expectation of total phase noise in PLL systems can be achieved. It can be seen from Figure 10 that the total noise from the passive lowpass filter is better than the active lowpass filter at low offset frequency region, 1 Hz to 33 kHz, while the active lowpass filter produces less total noise than the passive lowpass filter at the offset frequency higher than 33 kHz. In addition, those three total phase noises in this paper and the paper by Ducker (2000) reach the noise floor at the same magnitude of -155 dBc/Hz.

Conclusions

Detailed analysis and simulations of mathematical phase noise models of phase-locked loops have been presented. Unlike other existing phase noise models in which the filter noises are not included, this work has not only included the filter noises for the phase noise model but also compared the noise contribution between passive and active loop filters. The results show that simulations of phase noises without an inclusion of filter noises may not be accurate because the filter noises, particularly the active filter, significantly contribute to the total phase noise rather than other components. Moreover, the passive filter does not significantly dominate the phase noise at low offset frequency while the active filters entirely dominate. Therefore, the passive filter is a more efficient filter for PLL circuit at low offset frequency. The phase noise models presented in this paper are relatively simple and can be used for accurate phase noise prediction for PLL designs.

References

Dai, L. and Harjani, R. 2002. Design of Low-Phase-Noise CMOS Ring Oscillators, IEEE Transactions on Circuits and Systems II; Analog and Digital Signal Processing, Vol. 49; 328-338

Drucker, E. 2000. Model PLL Dynamics and Phase - Noise Performance, Microwaves & RF, May, 88-96.

Kroupa, V. F. 2003. Phase Lock Loops and Frequency Synthesis, John Wiley & Sons, Inc., New York., pp. 190-191.

Lathi, B.P. 1998. Modern Digital and Analog Communication System, 3rd Edition, Oxford University Press, New York., pp. 184-186.

Leeson, D.B. 1966. A simple model of feedback oscillator noise spectrum, Proceedings of the IEEE, Vol. 54; 329-330

Manassewitsch, V. 1987. Frequency Synthesizers Theory and Design, 3rd Edition, John Wiley & Sons, Inc., New York., pp. 105-114.

Misra, D.K. 2001. Radio-Frequency and Microwave Communication circuits, John Wiley & Sons, Inc., New York., pp. 75-77.

Razavi, B. 2001. Design of Analog CMOS Integrated Circuits, McGraw-Hill, London., pp. 100-101.

Rohde, U.L. 1997. Microwave and Wireless Synthesizers, John Wiley & Sons, Inc., New York., pp. 44-45,

Rohde, U.L., Poddar, A.K. and Bock, G. 2005. The Design of Modern Microwave Oscillators for Wireless Applications, John Wiley & Sons, Inc., New York., pp. 323-324.

Shu, Z., Lee, K.L. and Leung, B.H. 2004. A 2.4-GHz Ring-Oscillator-Based CMOS Frequency Synthesizer With a Fractional Divider Dual-PLL Architecture, IEEE Journal of Solid-State Circuits, Vol. 39; 452-462

Thamsirianunt, M. and Kwasniewski, T.A. 1997. CMOS VCO's for PLL Frequency Synthesis in GHz Digital Mobile Radio Communications, IEEE Journal of Solid-State Circuits, Vol. 32; 1511-1524

Zhang, B. Allen, P.E. and Huard, J.M. 2003. A Fast Switching PLL Frequency Synthesizer with an On-Chip Passive Discrete-Time Loop Filter in 0.25-µm CMOS, IEEE Journal of Solid-State Circuits, Vol. 38; 855 ñ 865

Appendix

Appendix A.1: Analytical treatments for Equations (10) and (11)

$$F_1(s)=\frac{V_{out1}(s)}{I_{in}(s)} = \frac{1}{sC_2}\left\|\left[R_1+\frac{1}{sC_1}\right]\right.$$

$$= \frac{1}{sC_2}\left\|\frac{1+sR_1C_1}{sC_1}\right.$$

$$= \frac{\frac{1+sR_1C_1}{s^2C_1C_2}}{\frac{1}{sC_2}+\frac{1+sR_1C_1}{sC_1}}$$

$$= \frac{1+sR_1C_1}{sC_1+sC_2+s^2R_1C_1C_2}$$

$$= \frac{1}{s}\left[\frac{1+sR_1C_1}{C_1+C_2+sR_1C_1C_2}\right]$$

$$= \frac{1+sR_1C_1}{s(C_1+C_2)(1+\frac{sR_1C_1C_2}{C_1+C_2})}$$

$$= \frac{k_{F1}(1+s\tau_{F1\_1})}{s(1+s\tau_{F1\_2})}$$

where $k_{F1} = 1/(C_1+C_2)$ is a constant. $\tau_{F1\_1} = R_1C_1$ and $\tau_{F1\_2} = (R_1C_1C_2)/(C_1+C_2)$ are time constants

Appendix A.2: Analytical treatments for Equations (13) and (14)

$$F_s(s)=\frac{V_{out2}(s)}{I_{in}(s)} = \left[\frac{\frac{1}{sC_2}\left\|R_1+\frac{1}{sC_1}\right.}{R_2}\right]$$

$$= \left[\frac{\frac{1}{sC_2}\left\|\frac{1+sR_1C_1}{sC_1}\right.}{R_2}\right]$$

$$= \frac{1}{R_2}\left[\frac{\frac{1+sR_1C_1}{s^2C_1C_2}}{\frac{1}{sC_2}+\frac{1+sR_1C_1}{sC_1}}\right]$$

$$= \frac{1}{R_2}\left[\frac{1+sR_1C_1}{sC_1+sC_2+s^2R_1C_1C_2}\right]$$

$$= \frac{1}{sR_2}\left[\frac{1+sR_1C_1}{C_1+C_2+sR_1C_1C_2}\right]$$

$$= \frac{1+sR_1C_1}{sR_2(C_1+C_2)(1+\frac{sR_1C_1C_2}{C_1+C_2})}$$

$$= \frac{(1+s\tau_{F2\_1})}{s\tau_{F2\_3}(1+s\tau_{F2\_2})}$$

where $\tau_{F2\_1} = R_1C_1$, $\tau_{F2\_2} = (R_1C_1C_2)/(C_1+C_2)$ and $\tau_{F2\_3} = R_2(C_1+C_2)$ are time constants in addition the DC gain of the active filter